Articles

Interaction of a Semirigid Agonist with *Torpedo* Acetylcholine Receptor†

Hideki Kawai,‡,§ Liren Cao,|| Susan M. J. Dunn,*,||,⊥ William F. Dryden,||,⊥ and Michael A. Raftery‡,▽

Department of Pharmacology, University of Minnesota Medical School, Minneapolis, Minnesota 55455, Department of Biochemistry, University of Minnesota, St. Paul, Minnesota 55108, and Division of Neuroscience and Department of Pharmacology, University of Alberta, Edmonton, Alberta, Canada T6G 2H7

Received September 15, 1999; Revised Manuscript Received December 20, 1999

ABSTRACT: The binding of the semirigid agonist [^{3}H]arecolone methiodide to the *Torpedo* nicotinic acetylcholine receptor has been correlated with its functional properties measured both in flux studies with *Torpedo* membrane vesicles and by single-channel analysis after reconstitution in giant liposomes. Under both equilibrium and preequilibrium conditions, the binding of arecolone methiodide is similar to that of other agonists such as acetylcholine. At equilibrium, it binds to two sites per receptor with high affinity ($K_d = 99 \pm 12$ nM), and studies of its dissociation kinetics suggest that each of these sites is made up of two subsites that are mutually exclusive at equilibrium. The kinetics of arecolone methiodide binding were monitored by the changes in the receptor intrinsic fluorescence, and the data are consistent with a model in which the initial binding event is followed by sequential conformational transitions of the receptor−ligand complex. In flux studies, arecolone methiodide was approximately 3-fold more potent ($EC_{50} = 31 \pm 5$ μM) than acetylcholine but its maximum flux rate was 4−10-fold lower. This phenomenon has been studied further by single-channel analysis of *Torpedo* receptors reconstituted in giant liposomes. Whereas the flexible agonist carbamylcholine (5 μM) was shown to induce channels with conductances of 56 and 34 pS with approximately equal frequency, arecolone methiodide (2 μM) preferentially induced the channel of lower conductance. These results are interpreted in terms of a simple model in which the rigidity of arecolone methiodide restrains the conformation that the receptor−ligand complex can adopt, thus favoring the lower conductance state.

The nicotinic acetylcholine receptor (nAChR)[1] from *Torpedo* electric organ is a pentameric glycoprotein composed of four homologous subunits in which two α subunits assemble with a β, γ, and δ subunit to form a transmembrane ion channel (*1*, *2*). Numerous equilibrium binding studies have suggested that each receptor oligomer carries two high-affinity binding sites for cholinergic agonists and competitive antagonists (*3*−*6*). In recent years, a variety of experimental approaches has been used to localize these binding sites and there is accumulating evidence for their occurrence at the interfaces between the α/γ and α/δ subunits (see ref *6*).

In a recent report (*7*), we provided evidence that the binding of agonists to these two high-affinity sites is complex. In studies of the kinetics of the dissociation of radiolabeled [^{3}H]ACh from the receptor complex, the dissociation rate was observed to increase in the presence of micromolar concentrations of unlabeled ligands. These results were interpreted in terms of a model in which each of the two high-affinity sites on the receptor is made up of two subsites (A and B) that are mutually exclusive at equilibrium. With the radiolabeled ligand initially occupying subsite A, occupancy of subsite B by unlabeled ligand reduces the affinity of the first site and accelerates the dissociation of radioligand. The dissociation of [^{3}H]SbCh was affected to a much lesser extent, and this led to the suggestion that this large bisfunctional ligand (Figure 1) may be able to bridge the two subsites or at least partially occlude the second subsite. These results, in conjunction with studies of the kinetics of association of a series of bischoline analogues having varying length (*8*), placed constraints on the physical distance between the two subsites.

The mechanisms by which the binding of an agonist to its receptor sites (or their subsites) lead rapidly to channel activation and more slowly to receptor desensitization are

† This work was supported by the Medical Research Council of Canada and the Graduate School, University of Minnesota Grants-in-Aid Program.

* To whom correspondence should be addressed: Department of Pharmacology, University of Alberta, Edmonton, Alberta, Canada T6G 2H7. Tel (780) 492 3414; Fax (780) 492 4325; E-mail Susan.Dunn@UAlberta.ca.

‡ Department of Pharmacology, University of Minnesota Medical School.

§ Present address: Department of Biology, 0357, University of California, San Diego, La Jolla, CA 92093.

|| Division of Neuroscience, University of Alberta.

⊥ Department of Pharmacology, University of Alberta.

▽ Department of Biochemistry, University of Minnesota.

[1] Abbreviations: ACh, acetylcholine; AChE, acetylcholinesterase; ANTS, 8-aminonaphthalene-1,3,6-trisulfonic disodium salt; α-BTx, α-bungarotoxin; Carb, carbamylcholine; DNPP, diethyl *p*-nitrophenyl phosphate; Hepes, *N*-(2-hydroxyethyl)piperazine-*N*′-2-ethanesulfonic acid; nAChR, nicotinic acetylcholine receptor; SbCh, suberyldicholine.

10.1021/bi992151o CCC: $19.00
Published on Web 03/16/2000

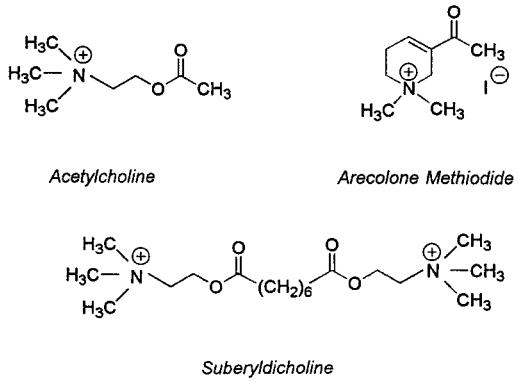

FIGURE 1: Structures of cholinergic agonists used in this study.

of fundamental significance. In this regard, fluorescence changes that accompany the formation of the receptor−ligand complex have been particularly useful in identifying receptor conformational changes that occur under preequilibrium conditions (see ref *8*). The observed kinetics have been invariably complex. In most cases, multiple conformational transitions have been detected and many complex binding mechanisms have been proposed (*8*−*10*). In general, however, the observed kinetics have been too slow to account for the rapidity of channel opening and they have been considered more likely to represent the conformational changes involved in receptor desensitization (*11*−*13*).

Studies of agonist binding to the nAChR have been complemented by ion flux measurements with isolated *Torpedo* membrane vesicles. By monitoring agonist-induced ion flux responses on rapid time scales, detailed information on both agonist potency and efficacy can be obtained (*14*). The sites involved in channel activation are of intrinsically low affinity. The EC_{50} for ACh-induced flux is approximately 80 μM (*15*), which is in agreement with the concentration dependence of nicotinic transmission at the neuromuscular junction (*16*). In flux studies, it has frequently been observed that different agonists display differences in their efficacies, i.e., they vary in the maximal flux rates that they can induce. Whereas "full" agonists, such as ACh and carbamylcholine, have maximal flux rates that can approach 1500 s^{-1} (*14*), other agonists, including SbCh (*17*), nicotine (*18*), and phenyltrimethylammonium (*12*, *18*), have much lower maximal rates of only 10−50 s^{-1}. In the absence of additional information, it has not been possible to interpret these observations at a molecular level.

Measurement of flux responses cannot approach the time resolution of single-channel events. Unfortunately, there have been few electrophysiological studies of *Torpedo* nAChR in situ, due largely to the fragility of isolated electroplax cells (*19*). There have, however, been a number of single-channel studies of native *Torpedo* receptors after reconstitution in planar bilayers (*20*−*23*), liposomes (*24*−*26*), and more recently in "giant liposomes" (*27*, *28*).

In the present study, we have investigated the binding and functional effects of a semirigid agonist, arecolone methiodide, which has been demonstrated to be a potent agonist at the frog neuromuscular junction (*29*−*31*). Whereas a flexible ligand such as ACh has been shown to change conformation upon binding to the nAChR (*32*), presumably adapting to the binding site, such conformational adaptation is restricted in arecolone methiodide. It may, therefore, be predicted that the flexibility of the ligand may dictate the type or extent of the receptor conformational change that it can induce.

We show here that the binding of arecolone methiodide under both equilibrium and kinetic conditions is similar to that of other agonists. In flux studies, arecolone methiodide was found to be approximately 3-fold more potent than ACh but its maximal flux rate was significantly lower. To investigate this phenomenon further, *Torpedo* membranes were reconstituted in giant liposomes (*27*, *28*) and patch clamp techniques were used to record single-channel events induced by application of arecolone methiodide or carbamylcholine (Carb). Although both ligands induced receptor desensitization and produced channels that have very similar lifetimes, interesting differences were revealed in their single-channel conductances. Carb (5 μM) induced two conductance states of 34 and 56 pS with approximately equal frequency. However, arecolone methiodide (2 μM) preferentially induced only the lower conductance state. These results are interpreted in terms of a simple model in which the rigidity of the arecolone methiodide restrains the receptor conformation to favor an open channel state with lower conductance.

EXPERIMENTAL PROCEDURES

Materials. The electric organs of *Torpedo californica* were from Aquatic Research Consultants (San Pedro, CA). The lyophilized venom of *Bungarus multicinctus* was obtained from Biotoxins (St. Cloud, FL). α-Bungarotoxin was purified and labeled with $Na^{125}I$ as previously described (*33*). Carbamylcholine chloride, acetylcholine chloride, and diethyl *p*-nitrophenyl phosphate (DNPP) were from Sigma Chemical Co. Suberyldicholine diiodide was from Aldrich, and 8-amino-1,3,6-naphthalenetrisulfonic acid disodium salt (ANTS) was from either Chem Service or Molecular Probes Inc. All other chemicals were of analytical grade.

Radiolabeled Ligands. [^{3}H]Acetylcholine iodide (specific activity = 46.9 mCi/mmol) was from DuPont-NEN Canada. [^{3}H]Suberyldicholine diiodide (batches of 166 and 74 mCi/mmol) was synthesized as described previously (see ref *7*). [^{3}H]Arecolone methiodide (108.9 mCi/mmol) was synthesized from 1-(1,2,5,6-tetrahydro-1-methyl-3-pyridinyl)ethanone hydrochloride (arecolone hydrochloride; a gift from Dr. John S. Ward, Lilly Research Laboratories, Indianapolis, IN). Briefly, an aqueous solution of arecolone hydrochloride was mixed with sodium bicarbonate−carbonate buffer (pH 10), titrated to pH∼10 with NaOH, and extracted three times with chloroform. The organic solution was dried over anhydrous magnesium sulfate twice and evaporated to yield an oily substance. This was reacted with slightly less than 1 equiv of [^{3}H]CH_3I (∼100 mCi/mmol, American Radiolabeled Chemicals, St. Louis, Mo) for complete reaction of the CH_3I. The crystalline product was washed with chloroform and dried in vacuo over phosphorus pentoxide and anhydrous calcium sulfate. Unlabeled arecolone methiodide was synthesized as above except that dichloromethane was used instead of chloroform. The concentration of stock [^{3}H]-arecolone methiodide solution was determined by its absorption spectrum at 223 nm ($\epsilon = 2.32 \times 10^4$ M^{-1} cm^{-1}). Its purity was examined by paper chromatography in 70% propanol. The resulting chromatogram was analyzed by three methods. First, a column of Whatman #1 paper was cut into pieces and counted for radioactivity. Second, iodine staining

of an identical column was performed. Third, the column was stained with the Dragendorff reagent (*34*) to identify the locations of amines. All methods identified one location, demonstrating the isotopic purity of the compound.

Preparation of nAChR-Enriched Membrane Fragments. nAChR-enriched membrane fragments were prepared from electric organs of *T. californica* as described previously (*35*) and were stored at −70 °C. Prior to use in binding experiments, the membranes were alkali-extracted to remove peripheral proteins (*36*, *37*) and, unless otherwise stated, were finally resuspended in Ca^{2+}-free *Torpedo* Ringers buffer (20 mM Hepes-Na^+, 250 mM NaCl, 5 mM KCl, 2 mM $MgCl_2$, and 0.02% NaN_3, pH 7.4). The concentration of [^{125}I]-α-BTx binding sites was determined by the DEAE-disk assay described previously (*38*), and membrane protein concentration was measured by either the Bio-Rad assay or the Lowry method (*39*). Specific activities of the membrane fragments were in the range of 2−4 nmol of [^{125}I]-α-BTx sites/mg of protein.

Equilibrium Radioligand Binding. Acetylcholinesterase activity in the membrane preparations was first inhibited by incubating concentrated membrane fragments (5−10 μM in α-BTx sites) for 3 min with 0.5% volume of 0.3 M DNPP prepared in 2-propyl alcohol and then diluting the membranes by approximately 5-fold in *Torpedo* Ringers buffer (20 mM Hepes-Na^+, 250 mM NaCl, 5 mM KCl, 4 mM $CaCl_2$, 2 mM $MgCl_2$, and 0.02% NaN_3, pH 7.4) and storing on ice until use. The equilibrium binding of [^{3}H]acetylcholine and [^{3}H]-arecolone methiodide was determined by a centrifugation method (*40*). Briefly DNPP-treated nAChR-enriched membranes were incubated with various concentrations of ^{3}H-ligand for 30 min at room temperature. Duplicate 50 μL aliquots were taken from each sample and counted for ^{3}H to give an estimate of total ligand concentration. The remaining samples were centrifuged for 20 min in an Eppendorf microcentrifuge at 13 000 rpm. Duplicate aliquots (50 μL each) were taken from the supernatant of each sample and counted for free ^{3}H-ligand. The amount of radioligand bound to nAChR was calculated by subtracting the free from the total ^{3}H-ligand concentration. Nonspecific binding was measured by including an excess of unlabeled ligand in parallel samples.

Equilibrium Competition Experiments. The ability of nonlabeled ligands to displace bound [^{3}H]arecolone methiodide or [^{3}H]acetylcholine was measured by first equilibrating DNPP-labeled nAChR preparations with radiolabeled ligand in the presence of various concentrations of competing ligands followed by determination of bound radioligand as described above. Data were normalized to the concentration of bound radiolabel measured in the absence of unlabeled ligand and were fit to a simple sigmoidal displacement curve equation by InPlot4 (GraphPad Software Inc.):

$$Y = A + \frac{B - A}{1 + [(10^X)^D/(10^C)^D]}$$

where Y is the fractional bound ^{3}H-ligand, A is the minimum fraction of bound ^{3}H-ligand in the presence of saturating concentrations of competing ligand, B is the fraction of bound ^{3}H-ligand in the absence of competing ligand, X is the log of the unlabeled ligand concentration, C is log IC_{50}, and D is the slope constant or "pseudo" Hill coefficient (n'). Inhibitory dissociation constants (K_i) were calculated from the Cheng−Prusoff correction (*41*):

$$K_i = \frac{IC_{50}}{1 + ([L]/K_d)}$$

where [L] is the concentration of radioligand in the assay and K_d is the equilibrium dissociation constant for the radioligand.

Measurement of Dissociation Kinetics. For measurements of radioligand dissociation on subsecond time scales, a Biologic rapid filtration system (Biologic, Meylan, France) was used (*7*). DNPP-treated membranes were first equilibrated with [^{3}H]ACh, [^{3}H]SbCh, or [^{3}H]arecolone methiodide for 30 min on ice. The AChR concentration was 0.25 μM in α-BTx binding sites, and concentrations of radioligand were chosen to ensure occupancy of >90% of these sites at equilibrium. For measurement of nonspecific binding, an excess of nonradiolabeled ligand was included in the equilibration mixture. Aliquots of 0.4 mL were applied to a Whatman GF/C filter mounted in the filtration apparatus and excess buffer was removed under vacuum. Dissociation of bound radiolabeled ligand was initiated by forced filtration for the desired time periods at appropriate flow rates with buffer alone or with the buffer containing various concentrations of unlabeled ligand. Times of filtration were 0.5−9 s and flow rates were varied from 2 to 0.5 mL/s to ensure adequate washing of the filter (*42*). After drying, the filters were counted for radioactivity in 4 mL of CytoScint to estimate the concentration of bound radioligand. Nonspecific binding was negligible at all time periods and was similar to that of radioligand alone without membranes.

The effect of the concentration of unlabeled ligand, [L], on the measured dissociation rate (k) was fit by:

$$k = k_0 + \frac{k_{max} - k_0}{1 + [(10^{\log EC_{50}})^n/(10^{\log [L]})^n]}$$

where k_0 is the apparent rate in the absence of an unlabeled ligand, k_{max} is the maximum dissociation rate, EC_{50} is the concentration of an unlabeled ligand that produces a half-maximal effect, and n is the pseudo Hill coefficient.

Stopped-Flow Measurements of the Kinetics of Ligand Association. The kinetics of ligand binding to AChR-enriched membrane preparations were measured by monitoring the changes in protein intrinsic fluorescence that occur upon ligand binding. These experiments were carried out using an Applied Photophysics SF.17MV microvolume stopped-flow spectrofluorometer apparatus equipped with a 150 W xenon arc lamp. Protein fluorescence was excited at a wavelength of 282 nm with a UV band-pass filter placed in the excitation beam to reduce stray light. Emission was recorded with a 300 nm cutoff filter. AChR-enriched membrane fragments in *Torpedo* Ringers buffer were rapidly mixed with ligand to give a final receptor concentration of 20 nM (in α-BTx binding sites). Fluorescence data were acquired and analyzed with an Archimedes computer and Applied Photophysics kinetic software. Each kinetic trace was fit by a two-exponential model:

$$F(t) = A_0 + A_1[\exp(-k_1 t)] + A_2[\exp(-k_2 t)] + k_0 t$$

where $F(t)$ is the fluorescence level at time t, A_0 is the equilibrium fluorescence level, k_1 and k_2 are the apparent rates of the two exponential processes, A_1 and A_2 are their corresponding amplitudes, and k_0 is the slope of the baseline used to correct for photolysis effects.

To improve the resolution of the biphasic kinetics, data were recorded using split time scales (e.g., 0.2 s/2 s, 2 s/20 s, 5 s/50 s) in which, for each trace, 200 data points were obtained over each time scale. Due to the small amplitude of the intrinsic fluorescence signals, data obtained in the first 100 ms were unreliable and were, therefore, eliminated from the analysis. Kinetic parameters obtained from phases whose half-lives contained fewer than 15 points were also excluded from further analysis. For mechanism fitting, the rate constants obtained from any phase in which the time scale of the reaction was less than 2.5 times or more than 25 times the half-life of that phase were also eliminated (see ref *40*).

Thallium(I) Flux Assays. The kinetics of agonist-mediated ion transport were measured by the stopped-flow fluorescence method previously described (*14*). Alkali-extracted *Torpedo* membrane vesicles were first loaded with the fluorescent probe ANTS. Extravesicular ANTS was removed by gel filtration on a Sephadex G-25 column equilibrated in 10 mM Hepes, pH 7.4, and 35 mM $NaNO_3$. The eluted membranes (1−2 μM in α-BTx binding sites) were used directly in stopped-flow measurements of Tl^+ uptake using the instrumentation described above. Briefly, membrane vesicles were rapidly mixed with agonist in a buffer in which the $NaNO_3$ was substituted by $TlNO_3$ and the rapid influx of Tl^+ was measured by its ability to quench the fluorescence of the entrapped dye. The rates (k_1) and amplitudes (A_1) of the flux responses were analyzed with a modified Stern−Volmer equation:

$$F(t) = \frac{A_1}{1 + KT_\infty(1 - e^{-k_1 t})} + k_0 t + A_0$$

where $F(t)$ is the fluorescence intensity at time t, K is the Stern−Volmer constant for Tl^+ quenching of the fluorophore (*14*), T_∞ is the concentration of Tl^+, k_0 is the rate of Tl^+ leak through the membrane, and A_0 is the fluorescence intensity at equilibrium.

Preparation of Giant Liposomes. Preparative procedures were modified from those described previously (*28*). L-α-Phosphatidylcholine (50 mg/mL) and CHAPS (1.5% w/v) were suspended in distilled water and kept at 4 °C overnight to allow dissolution. Aliquots of 0.5 mL were stored at −86 °C before use. *Torpedo* membranes were prepared as described above except that the final pellet was resuspended in dialysis buffer (10 mM Hepes-Na^+, pH 7.4, and 100 mM NaCl). Routinely, 400 μL of lipid−detergent mixture, 200 μg of membrane protein, and dialysis buffer were mixed to a final volume of 1 mL. After incubation for 1 h at 0 °C, the mixture was dialyzed exhaustively against dialysis buffer for 24 h. The sample was diluted in dialysis buffer and centrifuged at 100000*g* for 1 h. The resulting pellet was resuspended at 4 °C in 75 μL of dialysis buffer containing 5% (v/v) ethylene glycol by forcing the suspension through the needle of a small syringe until an apparently homogeneous suspension was obtained. The suspension was deposited as small droplets (~4 μL) on 3.5 cm diameter Petri dishes and allowed to partially dehydrate for 3 h at 4 °C in a desiccator containing anhydrous $CaCl_2$. The droplets were then rehydrated by addition of 4 μL of a 1:1 dilution of dialysis buffer in distilled water and incubated at 4 °C overnight in closed Petri dishes containing a wet paper towel on the bottom. The rehydrated drops were rinsed with experimental buffer (4 mM Hepes, pH 7.4, 50 mM NaCl, and 0.1 mM $CaCl_2$) and centrifuged at 1000 rpm for 10 min. The concentrated sample at the bottom of the centrifuge tube was diluted to a final volume of 1 mL in experimental buffer and stored at 4 °C.

Patch Clamp Recordings. Aliquots (75−100 μL) were pipetted onto 3.5 cm Petri dishes and incubated with 1 mL of experimental buffer for 5−10 min to allow the liposomes to deposit on the bottom of the dish. Single-channel recordings were obtained by use of patch-clamp techniques in the inside-out configuration as described by Hamill et al. (*43*). Experimental buffer was used both in the bath medium and in the electrode solution (referred to as "symmetrical" conditions). The electrode resistance was 5−25 MΩ when measured in experimental buffer. Single-channel recordings were obtained with electrode solutions containing either 5 μM Carb or 2 μM arecolone methiodide and an Axopatch-1D amplifier (Axon Instruments Inc., Foster City, CA). The holding potential was +65 mV, applied to the interior of the patch electrode (i.e., exterior of the receptor), and single-channel currents were monitored on an oscilloscope (Tektronix 5113, Beaverton, OR) and simultaneously recorded on magnetic tape.

Single Channel Analysis. All recorded signals were digitized (TL-1 DMA Interface, Axon Instruments) and analyzed by pClamp software (Version 5.5, Axon Instruments). Only single-channel events longer than 200 μs were used in the amplitude analysis. Open-channel events were plotted by fitting a Gaussian histogram to the current amplitude distribution (number of events versus current amplitude with bin width 0.1 pA) and the mean amplitude was obtained thereafter. The time constant (τ) for the open-channel state was determined by fitting of exponential plots to the frequency plot with a bin width of 1 ms.

RESULTS

Radiolabeled Ligands. Figure 1 shows the structures of the two flexible ligands, acetylcholine (ACh) and suberyldicholine (SbCh), and the semirigid nicotinic agonist, arecolone methiodide (*35*−*37*) used in this study.

Equilibrium Binding Experiments. The equilibrium binding of [^{3}H]ACh and [^{3}H]arecolone methiodide was measured in centrifugation assays. Each ligand bound with high affinity to two sites per receptor (i.e., equivalent to the number of sites for [^{125}I]-α-BTx) and there was no evidence for heterogeneity between these sites. The estimated K_d for [^{3}H]-ACh binding was 33.7 ± 3.5 nM (mean ± SEM) and [^{3}H]-arecolone methiodide bound with approximately 3-fold lower affinity (K_d = 99 ± 12 nM).

Equilibrium Displacement Experiments. Competition experiments were used to further characterize the equilibrium binding of arecolone methiodide. Both ACh and arecolone methiodide displaced bound [^{3}H]ACh, [^{3}H]arecolone methiodide, or [^{3}H]SbCh completely (Figure 2), indicating that these ligands compete for the same high-affinity sites at

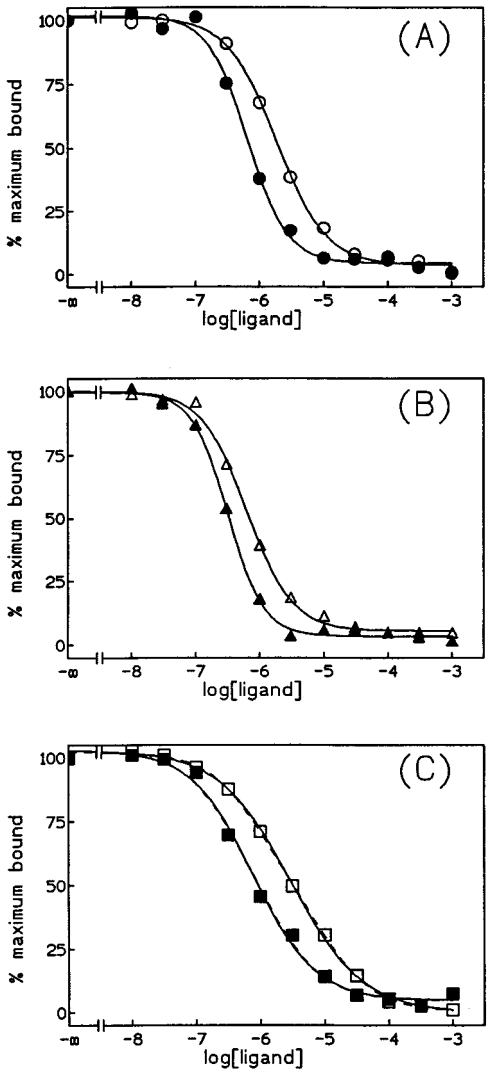

FIGURE 2: Equilibrium displacement of radiolabeled ligands. *Torpedo* membrane fragments (0.3−0.5 μM in α-BTx sites) were equilibrated with 0.3 μM radioligand and various concentrations of cold ligand, and the concentration of bound radioligand was determined by centrifugation assay. (A) Displacement of [^{3}H]-acetylcholine by acetylcholine (●) or arecolone methiodide (○). Curve-fitting as described in the text gave IC_{50} values of 0.76 μM (K_i = 77 nM) for acetylcholine and 2.14 μM (K_i = 216 nM) for arecolone methiodide with respective Hill coefficients (n') of 1.29 and 1.05. (B) [^{3}H]Arecolone methiodide displacement by either acetylcholine (▲) or arecolone methiodide (△). Curve-fitting gave values for acetylcholine of IC_{50} = 0.34 μM (K_i = 94 nM) and n' = 1.43, and for arecolone methiodide, IC_{50} = 0.74 μM (K_i = 0.205 μM) and n' = 1.05. (C) [^{3}H]Suberyldicholine displacement by either acetylcholine (■) or arecolone methiodide (□). Data fitting gave values for acetylcholine of IC_{50} = 1.01 μM (K_i = 0.106 μM) and n' = 0.85, and for arecolone methiodide, IC_{50} = 3.64μM (K_i = 0.38 μM) and n'= 0.75. Data shown are representative of three experiments carried out with similar results.

equilibrium. The affinity of arecolone methiodide was approximately 3-fold lower than that of ACh in displacing all three radioligands, as expected from the direct binding studies (see above). The larger values of K_i compared to the K_d values are due to the experimental conditions in which similar concentrations of radioligand and receptor were used, instead of the radioligand concentration being in excess of the receptor concentration, which will give K_i values similar to K_d values (*41*).

Table 1: Parameters Obtained from ^{3}H-Ligand Rapid Dissociation Kinetics[a]

	acetylcholine	arecolone methiodide
	[^{3}H]Acetylcholine	
EC_{50} (μM)	*2.09 ± 0.12*	1.24 ± 0.35
k_{1mM} (s^{-1})	*0.117 ± 0.006*	0.123 ± 0.12
k_0 (s^{-1})	*0.026 ± 0.012*	0.017 ± 0.015
	[^{3}H]Suberyldicholine	
EC_{50} (μM)	*15.3 ± 8.6*	1.04 ± 0.15
k_{1mM} (s^{-1})	*0.072 ± 0.006*	0.089 ± 0.069[b]
k_0 (s^{-1})	*0.029 ± 0.005*	0.011 ± 0.003
	[^{3}H]Arecolone methiodide	
EC_{50} (μM)	0.32 ± 0.15	0.64 ± 0.34
k_{1mM} (s^{-1})	0.328 ± 0.021[b]	0.330 ± 0.020[b]
k_0 (s^{-1})	0.0223 ± 0.0004	0.0300 ± 0.0028

[a] Parameters shown in italic type were from ref *7*. Parameter values listed represent mean ± SD. [b] K_{max} from sigmoidal curve-fitting was used.

Rapid Dissociation Experiments. We previously reported that the rate of dissociation of [^{3}H]ACh is accelerated by the presence of micromolar concentrations of unlabeled agonists (*7*; see introduction). In the present study, arecolone methiodide was found to display similar behavior. Following saturation of the high affinity sites by incubation of receptor (0.25 μM in α-BTx sites) with 0.5 μM [^{3}H]ACh or [^{3}H]-SbCh (sufficient to ensure >90% saturation of the two high-affinity sites), dissociation of the radioligand was induced by forced filtration of the labeled complex with buffer alone or in the presence of various concentrations of arecolone methiodide. By using the rapid filtration system, free and dissociated ligand are continually removed and this minimizes any possibility of rebinding during the dissociation reaction (*7*). On rapid time scales (0.5−9 s), dissociation was well described by a single-exponential process (data not shown) and arecolone methiodide accelerated the dissociation rate of [^{3}H]ACh in a similar manner (Table 1) to that previously observed for ACh, Carb, and SbCh (*7*). In agreement with previous results, the dissociation rate of [^{3}H]-SbCh was accelerated by arecolone methiodide but to a lesser extent (Table 1).

Dissociation Kinetics of [^{3}H]Arecolone Methiodide. The effects of unlabeled ACh and arecolone methiodide on the dissociation rate of [^{3}H]arecolone methiodide were also investigated (Figure 3). In these experiments the complex was first formed between 0.25 μM AChR (in α-BTx binding sites) and 2 μM [^{3}H]arecolone methiodide (in order to saturate at least 90% of the available binding sites). Semilog plots of the dissociation of the radiolabeled ligand were linear over the first 3 s of dissociation, and these data were used to approximate the apparent rate constants (see Table 1 and Figure 3). Over longer time periods, nonlinearity in the semilog plots became apparent (data not shown), suggesting that there may be some heterogeneity in either the binding sites for [^{3}H]arecolone methiodide and/or in the interaction between the subsites. This heterogeneity has not yet been investigated quantitatively but the data in Figure 3 clearly demonstrate that the dissociation of [^{3}H]arecolone methiodide is affected by the presence of unlabeled ligands in a manner similar to that of other agonists. Both the minimum and maximum rates observed were higher than those for [^{3}H]-ACh or [^{3}H]SbCh (Table 1), which is consistent with the

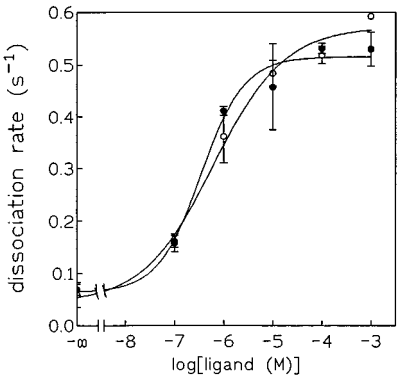

FIGURE 3: Effects of acetylcholine (●) and arecolone methiodide (○) on the initial rate of [^{3}H]arecolone methiodide dissociation. Rapid filtration techniques were used to measure dissociation on time scales of 0−3 s (see text for details). Parameters obtained from curve-fitting are given in Table 1.

approximately 3-fold lower affinity for this ligand (see above).

Kinetics of Arecolone Methiodide Binding Monitored by Intrinsic Protein Fluorescence. As reported previously (*44*, *45*), the binding of agonists to the membrane-bound nAChR can be monitored by changes in the intrinsic fluorescence of the receptor protein that result from complex formation. Rapid mixing of membrane fragments and arecolone methiodide resulted in concentration-dependent changes in protein fluorescence and the kinetics were clearly biphasic (Figure 4A). Figure 4 shows the ligand concentration dependencies of the rates of each of these phases averaged from four independent experiments. Both the fast and slow phases could be reasonably described by a hyperbolic model. These kinetics are very similar to those we have previously reported for the binding of SbCh to the nAChR when these were monitored by the fluorescence changes of an extrinsic fluorophore [5-(iodoacetamido)salicylic acid] that was covalently attached to the receptor protein close to the high-affinity sites (*13*; see Discussion). The data are consistent with a model (Scheme 1) in which the initial binding event is followed by sequential conformational changes of the bimolecular complex, RL. Parameters obtained from nonlinear regression fitting to Scheme 1 are given in the legend to Figure 4. The overall dissociation constant (*8*) is given by

$$K_{ov} = \frac{K_1 K_2 K_3}{1 + K_3(1 + K_2)}$$

and the estimated value of 0.045 μM is in reasonable agreement with the equilibrium dissociation constant (K_d = 0.099 μM) obtained in direct binding studies of [^{3}H]arecolone methiodide. This suggests that Scheme 1 provides a reasonable description of the conformational transitions leading to the high-affinity equilibrium state.

Scheme 1

$$R + L \overset{K_1}{\rightleftharpoons} RL \underset{k_{-2}}{\overset{k_2}{\rightleftharpoons}} R'L \underset{k_{-3}}{\overset{k_3}{\rightleftharpoons}} R''L$$

Measurement of Agonist-Induced Flux Responses. Arecolone methiodide was found to be a potent agonist of the *Torpedo* acetylcholine receptor. Figure 5 compares the flux response induced by arecolone methiodide and Carb by use of the Tl^+ flux stopped-flow method. The EC_{50} value for activation by arecolone methiodide was 31.3 ± 4.6 μM (mean ± sd). Thus arecolone methiodide is approximately 3-fold more potent than ACh (EC_{50} ~ 100 μM, *15*) and 30-fold more potent than Carb (EC_{50} ~ 1 mM, *14*). The maximum rate of flux induced by arecolone methiodide was, however, only about 60 s^{-1}, which is lower than that previously reported for the flexible agonists ACh (*15*) or Carb (*14*; see also Figure 5) but similar to the value reported for SbCh (*17*). Since we have found that the maximum flux rates are quite variable among different membrane preparations (unpublished observations), in the present study, control flux responses to 0.5 mM Carb were routinely measured and compared with those of arecolone methiodide. These control experiments have confirmed that the maximal flux rates induced by arecolone methiodide are 4−10-fold lower than those induced by Carb.

Single-Channel Recordings. Equilibrium dissociation constants for arecolone methiodide and Carb are comparable (99 vs 100 nM, *40*) but in functional assays, arecolone methiodide has been shown to be approximately 3−30-fold more potent than Carb (*14*, *29*, *30*; see also Figure 5) depending on the parameter of function employed. For the single-channel experiments a concentration of Carb (5 μM) was chosen empirically to avoid the bursting response interspersed with periods of desensitization that is characteristic of more saturating concentrations (*46*). Arecolone methiodide was used at a concentration of 2 μM, which is close to equipotency based on previous functional studies (*29*, *30*).

In every patch containing a responding receptor, transient currents were seen immediately when a holding potential of +65 mV was applied in the presence of either agonist. The currents spontaneously terminated over a periods that ranged from 1 to 34 min and this was interpreted as desensitization. There was no difference in the onset of desensitization between the two ligands and the time scales were similar to those reported previously for desensitization at the frog neuromuscular junction (*47*).

Figure 6 shows representative single-channel currents recorded in the presence of Carb or arecolone methiodide. While the Carb-induced currents clearly display a main conductance state and a frequent subconductance state, only the latter is seen with the arecolone methiodide-evoked currents. Excursions into a full amplitude current were rare. With the Carb-induced currents, transitions from one state to another were not uncommon, and the associated currents were treated as separate for the purposes of analysis. The distribution of current amplitudes is presented in Figure 7 together with the Gaussian fits superimposed. The relative frequencies of the two currents in each case can be seen. In the case of Carb, 42.9% of the evoked currents currents were at the lower amplitude, whereas 96.5% of the arecolone methiodide-evoked currents reflected the subconductance state. Point conductances of the two states were virtually identical (34 and 56 pS for the Carb-evoked currents and 33 and 58 pS for the arecolone methiodide currents).

Channel lifetime plots are illustrated in Figure 8. In the case of Carb, fitting by a double-exponential equation did not result in a significantly better fit than a single-exponential equation, which gave a time constant of decay (τ) of 1.96

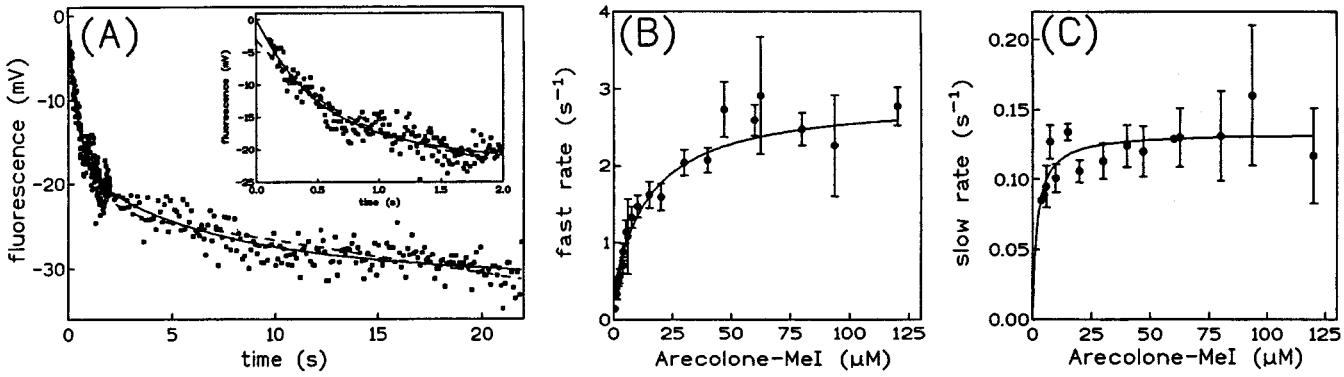

FIGURE 4: Kinetics of arecolone methiodide binding to *Torpedo* membranes measured by the quench in the intrinsic fluorescence of nAChR. (A) Representative kinetic trace obtained for the interaction between 7.5 μM arecolone methiodide and 20 nM AChR (in α-BTx sites). The trace was was analyzed by the sum of two exponential equations (solid line; $A_1 = 17.6$ mV, $k_1 = 2.18$ s^{-1}, $A_2 = 10.7$ mV, and $k_2 = 0.178$ s^{-1}) and a single-exponential equation (dashed line; $A_1 = 19.7$ mV and $k_1 = 1.18$ s^{-1}). (B, C) Concentration dependence of the apparent (B) fast and (C) slow rates for arecolone methiodide. The rates for each phase obtained from fitting by a two-exponential equation were pooled from four independent experiments and the data shown are the mean ± SEM concentration. According to Scheme 1, the concentration dependence of the faster phase is described by $k_{fast} = \{k_2[L]/(K_1 + [L])\} + k_{-2}$, while the apparent rate of the slower phase is approximated by $k_{slow} = \{k_3[L]/(K_1K_2)/(1 + [L]/K_1K_2))\} + k_{-3}$, (*65*). Solid lines are calculated by use of the best-fit parameters from nonlinear regression fitting: $K_1 = 15.9$ μM, $k_2 = 2.50$ s^{-1}, $k_{-2} = 0.38$ s^{-1}, $k_3 = 0.15$ s^{-1}, and $k_{-3} = 0.003$ s^{-1}.

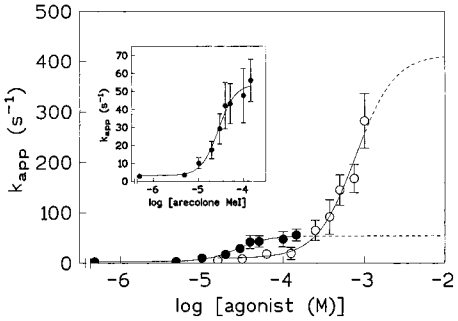

FIGURE 5: Effect of arecolone methiodide concentration on the apparent rate of Tl^+ flux (●) compared with the response induced by Carb (○). As reported previously (*14*), at higher Carb concentrations, the flux rate becomes too rapid for resolution by stopped-flow techniques. However, curve-fitting to the data obtained at Carb concentrations to 1 mM gave extrapolated values for the apparent equilibrium constant for activation (K_{act}) of 0.78 mM, a maximum flux rate (k_{max}) of 413 s^{-1}, and an apparent Hill coefficient (n') of 1.83. The inset shows the data for arecolone methiodide on an expanded scale; the best-fit values for K_{act}, k_{max}, and n' were 28.1 μM, 57.4 s^{-1}, and 2.35, respectively. Data shown are a representative concentration−effect curve and the error bars are standard errors of the mean (SEM) of multiple determinations made at each concentration.

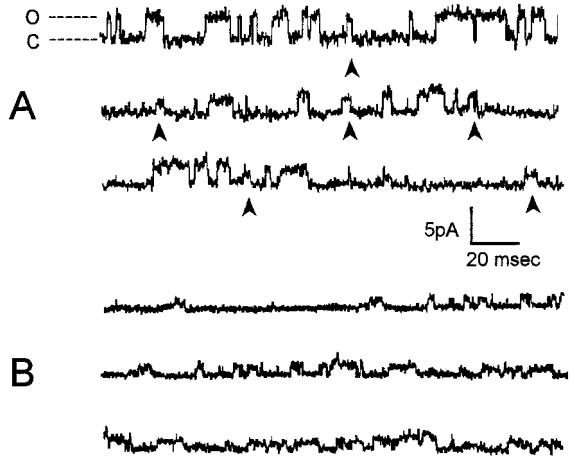

FIGURE 6: Typical single-channel currents from an inside-out patch recorded at a holding potential of +65 mV (applied to the interior of the electrode) filtered at 2 kHz. (A) Currents were measured in the presence of 5 μM carbamylcholine in a symmetrical buffer solution (see Experimental Procedures). Currents were a mixture of full conductance and subconductance events (arrowheads). (B) Currents measured in the presence of 2 μM arecolone methiodide. All the currents in the traces are from subconductance events.

ms. With the arecolone-evoked currents, the frequency plot was more obviously biphasic and a double-exponential fit gave τ values of 1.2 and 6.45 ms.

DISCUSSION

Arecolone methiodide (Figure 1) is one in a series of semirigid and potent cholinergic agonists that was first synthesized by Spivak et al. (*29*). From studies of the ability of arecolone methiodide to inhibit the initial rate of [^{125}I]-α-BTx binding to *Torpedo* nAChR (*31*), it was concluded that, under equilibrium conditions, arecolone methiodide has about 4-fold higher affinity than Carb and about 2-fold lower affinity than ACh. In the present study, we have synthesized [^{3}H]arecolone methiodide and direct binding studies have confirmed this earlier report. At equilibrium, [^{3}H]arecolone methiodide binds to two high-affinity sites per receptor molecule with an affinity approximately 3-fold lower than [^{3}H]ACh (see Results) and 2 times higher than previously reported values for [^{3}H]Carb (*40*). However, in flux studies (Figure 5), arecolone methiodide was found to be about 3-fold more potent than ACh (*15*) and 30-fold more potent than Carb (*14*). At high ligand concentrations, the maximum flux rate induced by the semirigid agonist was, however, much reduced compared to either ACh and Carb. In an attempt to explain these observations, we have carried out detailed studies of both the binding of arecolone methiodide to the *Torpedo* receptor and its receptor activation characteristics.

In most respects, the binding of [^{3}H]arecolone methiodide is similar to that of other agonists. It appears to bind to two high-affinity sites at equilibrium (see Results), and competition experiments (Figure 2) have suggested that arecolone competes with ACh and SbCh for binding to the same high-affinity sites on the receptor. Furthermore, studies of the kinetics of [^{3}H]arecolone methiodide dissociation suggest that, as for other agonists (*7*), each high-affinity site is

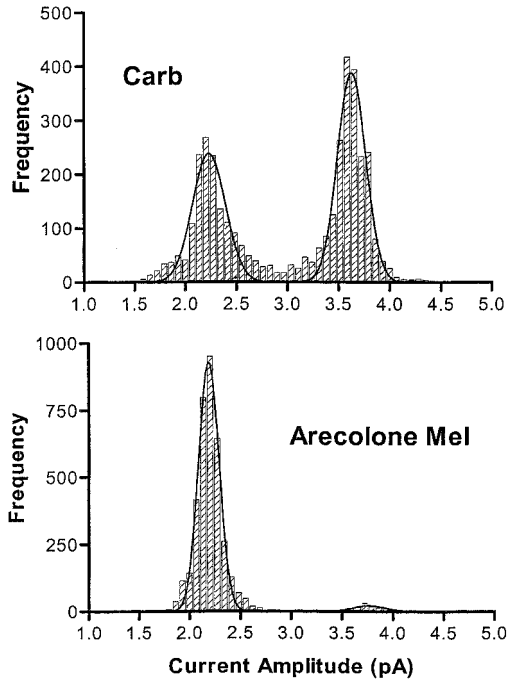

FIGURE 7: Frequency histograms of single-channel current amplitudes. Histograms have been fitted with Gaussian curves (solid lines). Mean current amplitudes evoked by Carb (±SD), measured at a holding potential of +65 mV, are 2.2 ± 0.2 and 3.6 ± 0.1 pA, and for arecolone methiodide the mean amplitudes are 2.2 ± 0.1 and 3.8 ± 0.2 pA. Data are derived from analysis of 3763 (Carb) and 3792 (arecolone methiodide) events.

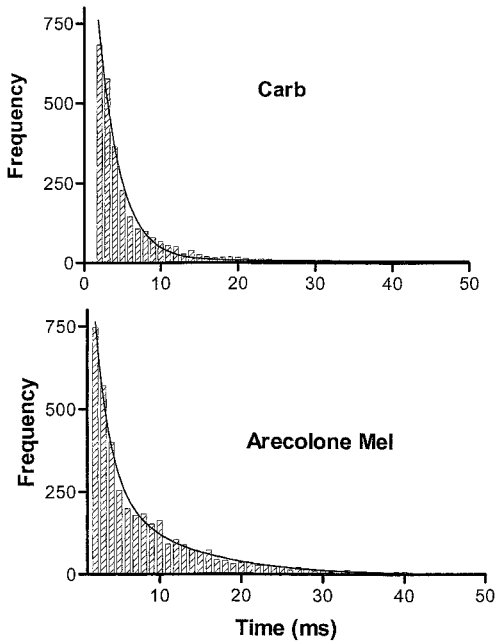

FIGURE 8: Frequency histograms of current duration plotted at 1 ms bin widths. The histograms have been fitted by double-exponential curves (solid lines). The double-exponential fit for the Carb distribution is only marginally better than a single exponential and a clear separation into two populations cannot be made with certainty, but for comparison with other authors, parameters derived from both are presented. The value of τ for Carb at +65 mV is 1.96 mV (single exponential) and 0.48 and 1.96 mV (double exponential). For arecolone methiodide, where the double-exponential decay is more unequivocal, the corresponding values for τ are 6.45 and 1.2 ms.

composed of two subsites that are mutually exclusive at equilibrium.

In early studies of arecolone methiodide binding, one unusual characteristic of this ligand was revealed (S. M. J. Dunn and M. A. Raftery, unpublished observations) and this prompted the current investigation. We have previously made extensive use of a fluorophore, 5-(iodoacetamido)salicylic acid (IAS), attached to α-subunit Cys192/193 near the high-affinity binding site (*13*, *40*) to monitor the kinetics of agonist binding to these sites. All agonists previously investigated enhanced the fluorescence of this probe and the kinetics revealed slow conformational changes that we suggested may reflect desensitization processes (*11*−*13*). Arecolone methiodide did not induce a change in IAS fluorescence and this led to the speculation that this ligand, unlike other agonists investigated to date, may not induce the changes in receptor conformation that lead to the desensitized state. We now demonstrate that this is not the case since single-channel analysis has confirmed arecolone methiodide-induced desensitization (see Results). The reasons for the lack of measurable IAS signal changes are currently under investigation.

The lack of an IAS signal change accompanying arecolone methiodide binding prompted the use of protein intrinsic fluorescence to measure its binding under preequilibrium conditions (Figure 4). The kinetics of arecolone methiodide binding were biphasic, with both phases having a concentration dependence and rate constants very similar to those we have described previously (*8*) for SbCh binding to IAS-labeled preparations. As reported by other authors (*44*, *45*), the amplitudes of the intrinsic fluorescence signals are small due to to the low intrinsic fluorescence of the receptor protein. However, the proposed scheme is consistent with kinetics previously observed for other ligands (see ref *8*), suggesting that the approach to equilibrium induced by arecolone methiodide is not significantly different from that induced by other agonists. Furthermore, this confirms that, in previous studies, the changes monitored by IAS have been a reliable measure of receptor conformational changes.

Although the binding of arecolone methiodide appears to be similar to that of ACh and Carb, there are obvious differences in the consequences of this binding. In functional studies, the predominant features of arecolone methiodide-induced responses were a reduced maximum rate of Tl^+ influx and a preponderance of subconductance channel openings. The Tl^+ influx data indicate that arecolone methiodide, like some other ligands (see introduction), is a partial agonist. In previous work with arecolone methiodide, this partial agonism was not evident since mainly normalized or comparative responses were reported (*29*−*31*).

The data in Figures 6 and 7 demonstrate that, at the concentrations of Carb (5 μM) and arecolone methiodide (2 μM) used, the subconductance state comprises a significant proportion of channel openings. Indeed, virtually the only state seen with arecolone methiodide is the subconductance state, and this is consistent with the diminished maximum Tl^+ influx rate that is observed with this ligand (see below). We have excluded the possibility that the larger currents seen with Carb are the result of the simultaneous opening of two channels in the same patch since they are not exact multiples of the lower current, and the frequency with which full current amplitude is attained directly from rest renders chance simultaneous opening of two independent channels improbable.

The subconductance state of the nAChR can be identified in many published records involving various ligands, and has been recognized as a real entity with peripheral nicotinic receptors from a variety of sources (*48*−*53*). Its significance, however, has been only tentatively discussed and it has no place in the kinetic schemes of receptor activation adopted by others in the field, despite early recognition that it deserves such a place (*48*).

Two clear and intriguing results of the present study are that (a) arecolone methiodide is a partial agonist as demonstated by its inability to induce the same maximum rate of Tl^+ flux as the full agonist Carb and (b) in single-channel recordings it favors a subconductance state. Qualitatively, the reduction in flux rate would be explained by its almost exclusive adoption of the subconductance state. Quantitative analyses of these phenomena require further experiments on the probability of channel opening and the concentration dependence of the distribution of open states In this regard, we have preliminary evidence (*54*) to show that the occurrence of the higher conductance state increases with Carb concentration. On the contrary, arecolone methiodide favors the subconductance state independently of concentration.

The single property that distinguishes the two ligands is the flexibility of the molecules. Increased incidences of subconductance states have been noted when more rigid ligands such as tubocurarine (*55*−*59*) or the nitromethylene insecticide imidacloprid (*60*) have been used. Carb is expected to undergo the same conformational change on binding as has been seen with ACh (*32*), a change that may be concomitant with the conformational transitions in the host receptor that are associated with activation and desensitization (*61*). In the case of arecolone methiodide and other ligands of limited flexibility, the receptor binding site may be precluded from undergoing a full conformational transformation and this may be manifested in the overwhelming incidence of subconductance states. Thus the subconductance state can be seen as associated with the initial stage of ligand binding, occurring before the transition that leads to the opening of a full conductance channel. This is over and above the already well-established dichotomy of channel open times, which are conventionally viewed as mono- and diliganded states in a two-binding-site model (*56*, *62*−*64*).

In a receptor assembly with two high-affinity binding sites but an undetermined number of low-affinity binding sites, such as has been proposed (*15*−*17*), it is possible to postulate more than two states of activation having different ionic conductances. Partial agonists, therefore, may be seen as ligands that favor the subconductance state of the receptor ion channel following occupation of the binding site.

ACKNOWLEDGMENT

We are grateful to Dr. John S. Ward, who provided us with arecolone hydrochloride. We thank David K. Okita (Minnesota) and Brian Tancowny (Alberta) for expert technical assistance.

REFERENCES

1. Raftery, M. A., Hunkapiller, M. W., Strader, C. D., and Hood, L. E. (1980) *Science 208*, 1454−1457.
2. Noda, M., Takanashi, H., Tanabe, T., Toyosato, M., Kikyotani, S., Furitani, Y., Hirose, T., Takashima, H., Inayama, S., Miyata, T., and Numa, S. (1983) *Nature 302*, 528−532.
3. McLane, K. E., Dunn, S. M. J., Manfredi, A. A., Conti-Tronconi, B. M., and Raftery, M. A. (1996) in *Protein Engineering and Design* (Carey, P., Ed.) pp 289−352, Academic Press Inc., New York.
4. Changeux, J.-P. (1995) *Biochem. Soc. Trans. 23*, 195−205.
5. Karlin, A., and Akabas, M. H. (1995) *Neuron 15*, 1231−1244.
6. Changeux, J.-P., and Edelstein, S. J. (1998) *Neuron 21*, 959−980.
7. Dunn, S. M. J., and Raftery, M. A. (1997) *Biochemistry 36*, 3846−3853.
8. Dunn, S. M. J., and Raftery, M. A. (1997) *Biochemistry 36*, 3854−3863.
9. Prinz, H. (1988) *Neurochem. Int. 12*, 109−119.
10. Ochoa, E. L. M., Chattopadhyay, A., and McNamee, M. G. (1989) *Cell. Mol. Neurobiol. 9*, 141−178.
11. Dunn, S. M. J., and Raftery, M. A. (1982) *Proc. Natl. Acad. Sci. U.S.A. 79*, 6757−6761.
12. Dunn, S. M. J., and Raftery, M. A. (1982) *Biochemistry 21*, 6264−6271.
13. Dunn, S. M. J., and Raftery, M. A. (1993) *Biochemistry 32*, 8608−8615.
14. Moore, H.-P. H., and Raftery, M. A. (1980) *Proc. Natl. Acad. Sci. U.S.A. 77*, 4509−4513.
15. Blanchard, S. G., Dunn, S. M. J., and Raftery, M. A. (1982) *Biochemistry 24*, 6258−6264.
16. Dreyer, F., Peper, K., and Sterz, R. (1978) *J. Physiol. (London) 281*, 395−419.
17. Kawai, H. (1998) Ph.D. Thesis, University of Minnesota, Minneapolis-St. Paul, MN.
18. Neubig, R. R., and Cohen, J. B. (1980) *Biochemistry 19*, 2770−2779.
19. Moreau, M., and Changeux, J.-P. (1975) *J. Mol. Biol. 106*, 457−467.
20. Montal M., Labarca, P., Fredkin, D. R. and Suarez-Isla, B. A. (1984) *Biophys. J. 45*, 165−174.
21. Nelson, N., Anholt, R., Lindstrom, J., and Montal, M. (1980) *Proc. Natl. Acad. Sci. U.S.A. 77*, 3057−3061.
22. Schindler, H. and Quast, U. (1980) *Proc. Natl. Acad. Sci. U.S.A. 77*, 3052−3056.
23. Schindler, H., Spillecke, F., and Neumann, E. (1984) *Proc. Natl. Acad. Sci. U.S.A. 81*, 6222−6226.
24. Anholt, R., Fredkin, D. R., Deernick, T., Ellisman, M., Montal, M., and Lindstrom, J. (1982) *J. Biol. Chem. 257*, 7122−7134.
25. Tank, D. W., Huganir, R. L., Greengard, P., and Webb, W. W. (1983) *Proc. Natl. Acad. Sci. U.S.A. 80*, 5129−5133.
26. Coronado, R., and Labarca, P. P. (1984) *Trends NeuroSci. 7*, 155−160.
27. Criado, M., and Keller, B. U. (1987) *FEBS Lett. 224*, 172−176.
28. Riquelme, G., Lopez, E., Garcia-Segura, L. M., Ferragut, J. A., and Gonzales-Ros, J. (1990) *Biochemistry 29*, 11215−11222.
29. Spivak, C. E., Waters, J., Witkop, B., and Albuquerque, E. X. (1983) *Mol. Pharmacol. 23*, 337−343.
30. Spivak, C. E., Gund, T. M., Liang, R. F., and Waters, J. A. (1986) *Eur. J. Pharmacol. 120*, 127−131.
31. Spivak, C. E., Waters, J. A., and Aronstam, R. S. (1989) *Mol. Pharmacol. 36*, 177−184.
32. Behling, R. W., Yamane, T., Navon, G., and Jelinsky, L. W. (1988) *Proc. Natl. Acad. Sci. U.S.A. 85*, 6721−6725.
33. Blanchard, S. G., Quast, U., Reed, K., Lee, T., Schimerlik, M. I., Vandlen, R., Claudio, T., Strader, C. D., Moore, H.-P. H., and Raftery, M. A. (1979) *Biochemistry 18*, 1875−1883.
34. Heftmann, E. (1967) *Chromatography*, 2nd ed., p 607, Reinhold Chemistry Textbook Series; Van Nostrand Reinhold, New York.
35. Elliott, J., Blanchard, S. G., Wu, W., Miller, J., Strader, C. D., Hartig, P., Moore, H.-P., Racs, J., and Raftery, M. A. (1980) *Biochem. J. 185*, 667−677.
36. Elliott, J., Dunn, S. M. J., Blanchard, S. G., and Raftery, M. A. (1979) *Proc. Natl. Acad. Sci. U.S.A. 76*, 2576−2579.
37. Neubig, R. R., Krodel, E. K., Boyd, N. D., and Cohen, J. B. (1979) *Proc. Natl. Acad. Sci. U.S.A. 76*, 690−694.

38. Schmidt, J., and Raftery, M. A. (1973) *Anal. Biochem. 52*, 349−354.
39. Lowry, O. H., Rosebrough, N. J., Farr, A., and Randall, R. J. (1951) *J. Biol. Chem. 193*, 265−275.
40. Dunn, S. M. J., Blanchard, S. G., and Raftery, M. A. (1980) *Biochemistry 19*, 5645−5652.
41. Cheng, Y.-C., and Prusoff, W. H. (1973) *Biochem. Pharmacol. 22*, 3099−3108.
42. DuPont, Y. (1984) *Anal. Biochem. 142*, 504−510.
43. Hamill, O. P., Marty, A., Neher, E., Sakmann, B., and Sigworth (1981) *Pflügers Arch. 391*, 85−100.
44. Bonner, R., Barrantes, F. J., and Jovin, T. M. (1976) *Nature 263*, 429−431.
45. Barrantes, F. J. (1978) *J. Mol. Biol. 124*, 1−26.
46. Sine, S. M., and Steinbach, J. H. (1987) *J. Physiol. 385*, 325−359.
47. Chesnut, T. J. (1983) *J. Physiol. 336*, 229−241.
48. Hamill, O. P., and Sakmann, B. (1981) *Nature 294*, 462−464.
49. Auerbach, A., and Sachs, F. (1983) *Biophys. J. 42*, 1−10.
50. Auerbach, A., and Sachs, F. (1984) *Biophys. J. 45*, 187−198; Brehm, P., Kidokoro, Y., and Moody-Corbett, F. (1984) *J. Physiol. 357*, 203-217.
51. Siegelbaum, S. A., Trautmann, A., and Koenig, J. (1984) *Dev. Biol. 104*, 366−379.
52. Colquhoun, D., and Sakmann, B. (1985) *J. Physiol. 369*, 501−557.
53. Kullberg, R., Owens, J. L., Camacho, P., Mandel, G., and Brehm, P. (1989) *Proc. Natl. Acad. Sci. U.S.A. 87*, 2067−2071.
54. Dunn, S. M. J., Cao, L., Jamshidi, H. R. and Dryden, W. F. (1999) *Soc. Neurosci. Abstr. 25*, 1721.
55. Trautmann, A. (1983) *J. Neural. Transm. Suppl. 18*, 353−361.
56. Takeda, K., and Trautmann, A. (1984) *J. Physiol. 349*, 353−374.
57. Morris, C. E., and Montpetit, M. (1986) *Can. J. Physiol. Pharmacol. 64*, 347−355.
58. Morris, C. E., Montpetit, M. R., Sigurdson, W. J., and Iwasa, K. (1988) *Can. J. Physiol. Pharmacol. 67*, 152−158.
59. Strecker, G. J., and Jackson, M. B. (1989) *Biophys. J. 56*, 795−806.
60. Nagata, K., Aistrup, G. L., Song, J.-H., and Narahashi, T. (1996) *Neuroreport 7*, 1052−1028.
61. Castresana, J., Fernandez-Ballester, G., Fernandez, A. M., Laynez, J. L., Arrondo, J.-L., Ferragut, J. A., and Gonzalez-Ros, J. M. (1992) *FEBS Lett. 314*, 171−175.
62. Labarca, P., Lindstrom, J., and Montal. M. (1984) *J. Gen. Physiol. 83*, 473−496.
63. Sine, S. M., and Steinbach, J. H. (1986) *J. Physiol. 373*, 129−162.
64. Edmonds, B., Gibb, A. J., and Colquhoun, D. (1995) *Annu. Rev. Physiol. 57*, 469−493.
65. Quast, U., Schimerlik, M. I., and Raftery, M. A. (1979) *Biochemistry 18*, 1891−1901.

BI992151O